ELSEVIER

Plasmonic nanoparticle-based epoxy photocuring: A deeper look

Adam T. Roberts [1,†,‡], Jian Yang [2,‡], Matthew E. Reish [3], Alessandro Alabastri [4], Naomi J. Halas [2,4,5], Peter Nordlander [2,4], Henry O. Everitt [1,4,*]

[1] U.S. Army Aviation & Missile RD&E Center, Redstone Arsenal, AL 35898, USA
[2] Dept. of Physics and Astronomy, Rice University, Houston, TX 77005, USA
[3] Oak Ridge Institute of Science and Education, Redstone Arsenal, AL 35898, USA
[4] Dept. of Electrical and Computer Engineering, Rice University, Houston, TX 77005, USA
[5] Dept. of Chemistry, Rice University, Houston, TX 77005, USA

Many epoxy adhesives require high temperatures to bond composite materials. However, oven heating severely restricts what may be attached or enclosed within composite material-based structures and greatly limits the possibilities for repair. Inspired by initial reports of photothermal epoxy curing using plasmonic nanoparticles, we examine how laser-illuminated Au nanoparticles embedded within high-temperature epoxy films convert the conventional thermal curing process into a photothermally driven one. Our theoretical investigations reveal that plasmonic nanoparticle-based epoxy photocuring proceeds through a four-stage process: a rapid, plasmon-induced temperature increase, a slow localized initialization of the curing chemistry that increases the optical absorption of the epoxy film, a subsequent temperature increase as the epoxy absorbs the laser radiation directly, and a final stage that completes the chemical transformation of the epoxy film to its cured state. Our experimental studies validate this model, and also reveal that highly local photocuring can create a stronger bond between composite materials than thermal curing without nanoparticles, at times even stronger than the composite material itself, substantially reducing the time needed for the curing process. Our findings support key advances in our understanding of this approach to the rapid, highly efficient bonding and repair of composite materials.

Introduction

The need to reduce the weight of large systems such as vehicles and aircraft for improved performance has led to the widespread adoption of composite materials to replace metals [1–3]. Unlike metals, which are primarily worked in an unheated state, composite materials frequently require heating as part of the assembly process. For example, heat-cured thermoset composites are formed, then cured in an oven, while thermoplastic composites are melted, then pressed into final form. For repairs, high-temperature epoxy is frequently used to bind composite materials, which requires oven heating [1,2]. However, reheating a formed composite to bond additional material onto it can significantly degrade the quality of the original material [4]. Complex composite-based systems frequently contain sensitive components, such as electronics or sensors, which cannot typically survive the high temperatures of oven curing. Effective approaches for controlling the thermal processing of composites for streamlined assembly and repair, especially ones that preserve the

* Corresponding author at: U.S. Army Aviation & Missile RD&E Center, Redstone Arsenal, AL 35898, USA.
E-mail address: Everitt, H.O. (Henry.Everitt@rice.edu).
† Now at Northrup Grumman, Redondo Beach, CA, USA.
‡ Contributed equally.

https://doi.org/10.1016/j.mattod.2018.09.005

integrity of the material and any associated components, are critically needed.

The controlled deposition of heat into a highly localized area to weld a thermoplastic, cure a thermosetting polymer, or bond composites with high temperature epoxy would be a transformative advance in the field of composite materials [5,6]. Photothermal heating of composite materials by lasers represents one possible solution, especially for composites that are at least partially transparent over a specific wavelength region: illumination by a laser source operating in this spectral window could heat buried junctions and enable localized epoxy curing. If two different composite materials are being joined, it is preferable for the heat to be generated only at the interface between the two materials, which can be accomplished by placing a bonding material designed to absorb laser radiation at that junction [7,8]. It has recently been shown that gold nanoparticles, possessing an intense optical absorption corresponding to their plasmon resonance, can, through light absorption and localized photothermal heating, enable epoxy curing *in situ*. Because this light-based bonding process has such broad potential across fields ranging from biomedicine to vehicle repair, it is worthwhile to examine this process in detail, and to speculate whether the process itself may depend upon the type of materials to be bonded and/or the specific properties of the cross-linking epoxy host.

Inspired by these initial studies [7,8], we have performed a detailed examination of the plasmonic particle-based epoxy photocuring process. By incorporating Au nanoparticles (NPs) into a high-temperature epoxy, resonant laser illumination can very effectively induce photothermal curing. When illuminated with resonant light, metallic nanoparticles that support localized surface plasmons possess an optical cross section far greater than their physical cross section and are well known to behave as highly efficient light-to-heat converters [9–14]. While initial studies examined laser curing of a liquid epoxy by plasmon nanoparticle-based photothermal heating to temperatures above the curing temperature[8], we examine a different regime, where laser illumination can initiate and accelerate curing well below the threshold for photoinduced curing in the absence of the nanoparticles, and well below laser powers that would induce surface charring of the bonded composite materials. Au NPs, whose plasmon resonance coincides with both the laser wavelength and the transparency window of a composite material, concentrate heat in precisely the location where they are positioned. A low-power laser beam scanned over a 5-cm^2 region cures the epoxy with equivalent bond strength but in less time and more locally than is possible by conventional (oven-based) curing. In the regime studied here, the laser-heated nanoparticles are used to increase the absorption coefficient of the binding epoxy material itself during curing, providing a positive feedback mechanism that triggers a rapidly advancing, self-sustained cure front that propagates until the curing process is complete. We observe that composite materials bonded by this process show an undiminished bond strength relative to the material strength of the pristine composite material itself.

To understand these behaviors and identify optimal experimental conditions, we introduce a theoretical model that incorporates the induced changes in the optical properties of the epoxy during the photocuring process, as well as the photothermal response and heat transport in the composite-epoxy system. This model, validated by experimental measurements, supports our interpretation of the complex chemical transformation observed during the photocuring process. Initially, laser illumination rapidly heats the nanoparticles, then the hot nanoparticles initiate epoxy curing locally, during which time the optical absorption coefficient of the epoxy increases, which then allows the epoxy to absorb the illumination directly, precipitating a cure front that rapidly heats and cures the entire epoxy film. This highly desirable, theoretically predicted, and experimentally demonstrated NP-induced change in the optical properties of the (epoxy) host fundamentally distinguishes our work from prior work (e.g. [8,14,15]) and addresses a wider class of problems for which thermal modifications of a material's dielectric function profoundly affect its photothermal behavior. Our analysis shows how curing time may be influenced by laser power and NP density, indicating tradeoffs between power, cost, and speed for optimizing this process. This theoretical model may be applied to any nanoparticle-doped host medium whose dielectric function can change during laser illumination [7,8], expanding the applicability of nanoparticle-based photothermal processing to other areas of manufacturing where local photothermal materials modification may be of potential importance.

Materials and methods

Epoxy optical properties before and after curing

This study employed a thin heat-cured adhesive epoxy film (FM 300, Cytec Engineered Materials) widely used in metal-to-metal, metal-to-composite, and composite-to-composite bonding. For conventional thermal curing, this translucent, green-colored epoxy cures in an hour at $T_c = 177$ °C (350 F), changing color and opacity as it hardens by the thermally activated cross linking of polymers that produce a high strength bond. [16]. To characterize its temperature-dependent absorption spectrum, a 0.2-mm-thick film of FM 300 was pressed onto glass microscope slides and cured on a hot plate following the manufacturer's specified curing cycle. Optical absorption measurements of the epoxy before and after thermal curing are shown in Fig. 1a, along with photographic images of the uncured and cured samples. The uncured film exhibits an absorption minimum near 500 nm, absorbing only 50% of the light from a 10-W frequency-doubled Nd:YAG laser operating at 532 nm (Sprout by Lighthouse Photonics). That minimum disappears as the film cures: in its cured state, the epoxy film absorbs up to 90% of 532-nm incident light.

To enhance the laser absorption of the uncured film, 40-nm diameter spherical Au NPs (Sigma Aldrich 753637-100ML) were used. A transmission spectrum of the Au NPs in a solution of 0.1 mM phosphate-buffered saline (PBS) in a 1-mm path length cuvette was obtained (Fig. 1b). The NPs exhibited a narrow plasmonic absorption peak centered at 530 nm that coincided with the 532-nm laser wavelength. Samples were composed of different NP concentrations deposited onto the surface of a glass slide onto which the epoxy film was subsequently pressed (at 140 psi for 10 min at room temperature). The suspended NPs were drop cast onto the substrate, then heated to 40 °C to evaporate the solvent and minimize NP aggregation. NP concentration was

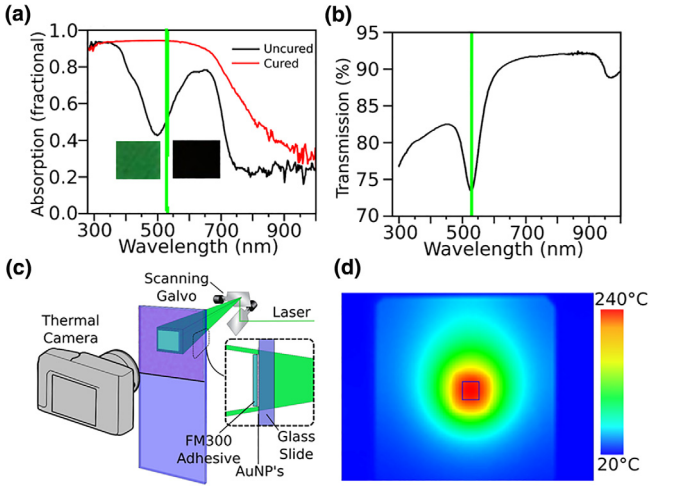

FIGURE 1

Epoxy optical absorption and experimental setup. (a) Optical absorption spectra of FM 300 epoxy film before and after curing, with corresponding photographic images (Inset: left image, before curing; right image, after curing). (b) Transmission spectrum of Au NPs in solution. In both (a) and (b), the vertical green line corresponds to the 532-nm laser wavelength. (c) Layout of the test system for laser scanning and IR video temperature measurement. Inset: cross-section of sample geometry. (d) IR temperature video frame showing the 1″ × 1″ microscope slide (light blue) coated with Au NPs and FM 300 epoxy film. The reported temperature represents an average of the 2.5 × 2.5-mm black box, denoting the laser-scanned area of the epoxy film.

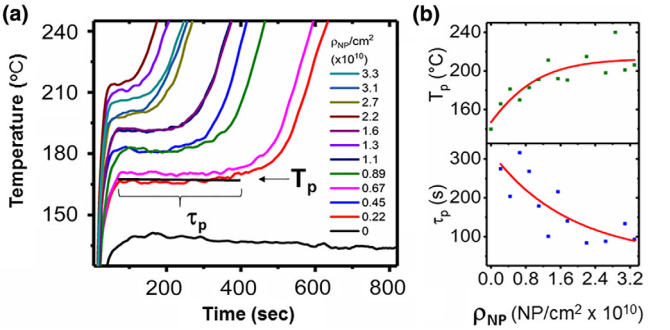

FIGURE 2

Experimental results of accelerated photocuring. (a) Temporal evolution of the temperature measured for increasingly NP-doped FM 300 epoxy film samples under constant laser illumination (5 W/cm^2, 532 nm laser wavelength). (b) The measured plateau temperature T_p and plateau time τ_p as a function of nanoparticle concentration ρ_{NP}, overlaid by an Arrhenius-type data analysis (red lines), shows a nonlinear increase in T_p and decrease in τ_p along with sample-to-sample variability.

easily selected by controlling the titrated volume of the suspended NPs.

Photocuring of doped epoxy films

To photocure the epoxy film, the ~1-mm diameter unfocused laser beam was rapidly raster-scanned across the sample (Fig. 1c) in either a 100 Hz × 130 Hz Lissajous or sawtooth pattern for uniform light distribution over a user-defined region. Although at full power the intensity of the spot exceeded 1 kW/cm^2, the average laser intensity I_L experienced by the samples as the 4.25-W spot rapidly scanned over a 9-mm × 9-mm region was approximately 5 W/cm^2. Since the curing reaction happens at a much slower time scale than the laser scan period, this effective-intensity-approach is valid and used in later discussions. The uniform heating produced by the rapidly scanning spot is confirmed by burn cards and an infrared (IR) camera (FLIR model T450sc) that monitored and recorded the laser heating of each sample as a video whose frames captured the time-evolving thermal distribution (Fig. 1d). The IR images obtained of the sample under illumination reveal a relatively abrupt drop in temperature outside the laser scanned area because of the low thermal conductivity of the film and glass.

These measurements revealed how the specific temperature dynamics of the photocuring process depended on both nanoparticle density and laser intensity. A series of samples was prepared with nanoparticle concentration ρ_{NP} ranging from 0 to 3.3×10^{10} NP/cm^2, and the photocuring dynamics was recorded for each sample (Fig. 2a). Each measurement was stopped either at 1000 s or once the sample temperature rose above 250 °C (475 F) to avoid scorching. Even with no NPs, the intrinsic optical absorption of film initially causes its temperature to rise, but under these conditions the film never reaches the curing temperature, and heat-induced flow of the epoxy smooths the surface, reduces scatter, and causes the temperature to decrease slowly. When NPs were added, all of the films cured: each experienced a rapid initial temperature rise, followed by a plateau of duration τ_p that decreased with increasing ρ_{NP} and a plateau temperature T_p that increased with increasing ρ_{NP}. After the plateau, the temperature of the epoxy film again rose rapidly as it cured. Fig. 2b summarizes the plateau temperatures T_p and plateau times τ_p of these epoxy films as a function of Au NP concentration. The significant variabilities in T_p and τ_p with increasing ρ_{NP} observed are most likely due to random aggregations of the NPs when deposited on the glass surface: the presence of Au NP aggregates reduces the number of localized photothermal "hot spots" and slows photocuring. As a guide, an Arrhenius-type rate function was used to analyze the data; it indicated a decreased acceleration in temperature growth for $\rho_{NP} > 1.7 \times 10^{10}$ NP/cm^2 and no significant reductions in curing time for $\rho_{NP} > 2 \times 10^{10}$ NP/cm^2. With high ρ_{NP}, the epoxy films cured in 100 s or less, in striking contrast to the case without Au NPs where curing did not occur even after 1000 s of laser illumination under identical conditions.

Theoretical model

A two-part theoretical model was developed (Finite Element Method, COMSOL Multiphysics 5.2a) to simulate the plasmonic nanoparticle-based photocuring process (Fig. 3). The first part considers the electromagnetic interaction between the incident laser beam and a 2-dimensional array of Au NPs whose interparticle distances match the experimental average distance between NPs. The optical absorption and transmission were calculated, along with the Joule heating produced by resonant illumination. This part of the calculation describes the dependence of film heating on ρ_{NP}. The second part takes as input the heat generated by the plasmonic NPs and the optical transmission of the array to calculate how heat diffuses into the epoxy film while curing and

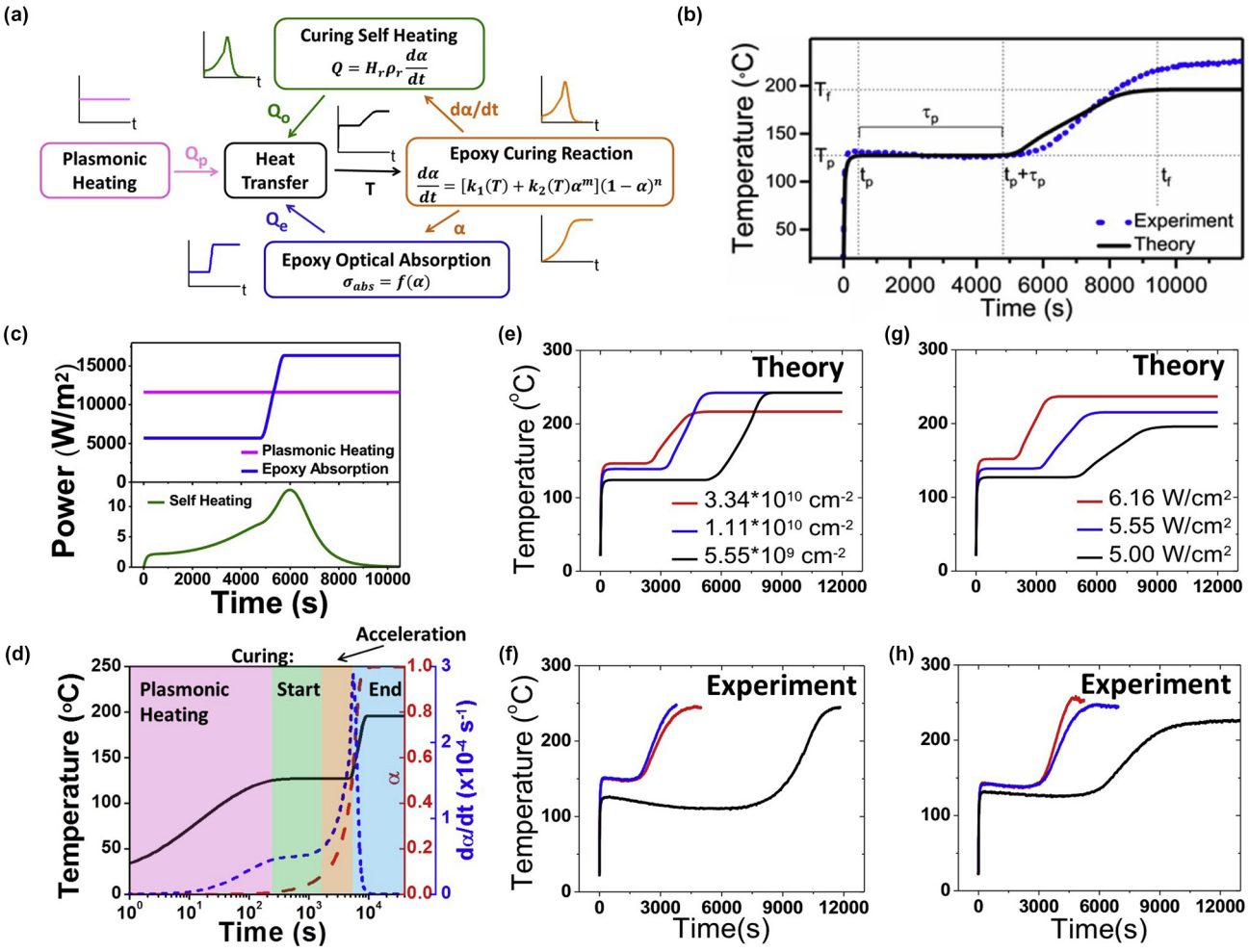

FIGURE 3

Theoretical model and comparison with experiments. (a) Schematic of the plasmonic nanoparticle-accelerated curing process: three different heating sources – Plasmonic Heating (pink), Curing Self Heating (green) and Epoxy Optical Absorption (blue) – serve as input for the equations of the Heat Transfer module (black) which solves for the temperature that, at each time step, is input to the Epoxy Curing Reaction equation (orange). (b) Comparison between experimental results (dotted blue) and theoretical calculations (solid black) for the temperature increase of a FM 300 epoxy film sample over time. An input power of P_{in} = 5 W/cm^2 and a nanoparticle density ρ_{NP} = 2.2 × 10^{10} NP/cm^2 are considered. (c) Heating power produced by all three mechanisms, plasmonic heating, optical absorption, and self-heating from the exothermic nature of the cure reaction, plotted as a function of time to correlate with the theory and experimental data in b. (d) Temperature (solid black), curing state (dashed red) and curing rate (dotted blue) dependence on time (log scale), based on conditions intended to correlate with behavior observed in b. The overall process is divided into four regions. (i) *Plasmonic heating* (pink) with a fast temperature rise, (ii) *Initial curing phase* (green) where the curing state begins to increase, (iii) *Acceleration phase* (tan) which shows the peak of the curing rate and (iv) *Final curing phase* (blue) featuring a completed curing process and a constant final temperature. (e) Theoretical and (f) experimental dynamics of the photocuring process as a function of ρ_{NP} (black: 5.5 × 10^9 NP/cm^2; blue: 1.11 × 10^{10} NP/cm^2; red: 3.34 × 10^{10} NP/cm^2. Laser intensity: 6 W/cm^2). (g) Theoretical and (h) experimental dynamics of the photocuring process as a function of laser intensity (ρ_{NP} = 2.2 × 10^{10} NP/cm^2. Black: 5.00 W/cm^2; blue: 5.55 W/cm^2; red: 6.16 W/cm^2).

how optical power is absorbed by the epoxy itself. Both phenomena contribute to the temperature increase of the film. In addition, the substantial change in optical absorption by the epoxy during the curing process is also taken into account, while the commensurate damping of the plasmon resonance was found to be negligible and could be omitted.

The curing dynamics are described by [17–19]

$$\frac{d\alpha}{dt} = (k_1 + k_2\alpha^m)(1-\alpha)^n, \quad (1)$$

where

$$k_i = A_i \exp\left(-\frac{E_i}{RT}\right), \quad (2)$$

$d\alpha/dt$ is the curing rate, α is the time-dependent curing fraction (spanning 0 for no cure to 1 for fully cured), t is time, k_i are rates for the material-specific thermally activated processes characterized by activation energies E_i and rate constants A_i [20], R is the gas constant, T is time-evolving temperature, and m and n are material-specific exponents related to the reaction order [21,22]. While some of these parameters have been established for certain epoxies [17], they are currently unknown for the FM 300 epoxy used in these studies. These empirical parameters, together with the heat conduction coefficient of the epoxy and the heat transfer coefficient between the system and air, may be estimated by analyzing the experimental data. Reasonable values have been found for all these parameters (see Appendices A–C for details).

The theoretical model is schematically described in Fig. 3a. A separate calculation is first performed to obtain the plasmonic heating for a specific I_L and ρ_{NP} (see Appendices A and B). At the interface between the glass slide and the epoxy film, the electromagnetic dissipation (pink block) produces a constant plasmonic heating power Q_P that is utilized as input for the heat transfer (black block) and curing (orange block) equations. Additional heat sources derive from the evolving optical absorption of the epoxy film Q_E (blue block) and by the (small) exothermic curing self-heating reaction Q_S (green block). The optical absorption of the epoxy film is calculated by the curing equation and, being dependent on α, has different values across its volume. Q_S depends primarily on the curing rate $d\alpha/dt$, weighted by the mass density of the epoxy film ρ_r and the enthalpy of the reaction H_r.

Results and discussion

Photocuring process for doped epoxy films

Fig. 3b presents typical data obtained for a NP density of $\rho_{NP} = 2.22 \times 10^{10}$ NP/cm^2, directly compared with the output of our theoretical model for the same NP density and experimental conditions. The rapid rise in temperature is followed by a long plateau at t_p with duration τ_p, at which the temperature T_p remains relatively constant but below the curing temperature T_c. Then, rather unexpectedly, the temperature starts to rise again at $t_p + \tau_p$, climbing above T_c before reaching an even higher temperature plateau T_f at t_f. Soon the epoxy film is fully cured, and the laser must be turned off to prevent charring of the epoxy film. The rates, temperatures, and time scales associated with each of these behaviors were found to depend on ρ_{NP}, laser intensity I_L, and ambient conditions.

The combined effect of the three heating sources Q_E, Q_S, and Q_P is plotted in Fig. 3c. The intrinsic absorption Q_E is initially smaller and eventually larger than the constant plasmonic heating Q_P, but overall they are on the same order of magnitude. Compared to Q_E and Q_P, the curing reaction gives a negligible heating Q_S. In this manner both $\alpha(t)$ and $d\alpha/dt$ are estimated, from which Q_E and Q_S are respectively calculated (details about the relevant parameters can be found in Appendices B and C). An extinction function $\sigma_{abs}(\alpha)$ expresses the increased absorption of the epoxy film with increasing α and produces the temporal evolution of Q_E plotted in Fig. 3c. This function is constrained by the experimentally measured extremes $\sigma_{abs}(0)$ and $\sigma_{abs}(1)$ derived from the epoxy absorption spectrum shown in Fig. 1a (details about $\sigma_{abs}(\alpha)$ are provided in Appendix B).

The photocuring process can be divided into four phases (Fig. 3d):

- *Plasmonic heating*. During this initial phase (pink region), the laser causes a rapid temperature increase of the NPs and the surrounding epoxy film, which then reaches a plateau of T_p (~130 °C) at t_p (~100 s) as the NPs come into thermal equilibrium with their surroundings (black solid line). Eq. (2) indicates how the reaction rates $k_1 \propto e^{-E_1/k_BT}$ and $k_2 \propto e^{-E_2/k_BT}$ increase with temperature because of the exothermic nature of the cross-linking curing reaction [17].
- *Initial curing phase*. Following equilibration of the heated NPs, the first temperature plateau (green region) is reached and maintained at T_p for τ_p (between 300 and 5000 s). Eq. (1) captures how the cure state α of the epoxy film (red dashed line) begins to increase during this temperature plateau. Although Eq. (1) indicates that the relationship between the curing rate $d\alpha/dt$ (blue dotted line) and cure state α can be rather complex, in this regime a small α produces a small curing rate $d\alpha/dt$.
- *Acceleration*. After τ_1 (between 5000 and 10,000 s), the cure state α has grown large enough so that the curing rate $d\alpha/dt$ is significant. In this regime (tan region), the rapid curing of the epoxy increases its intrinsic optical absorption and the temperature increases again.
- *Final curing phase*. When the heat generated in both the plasmonic NPs and the epoxy film is balanced by heat dissipation into the background through conduction and convection, a new temperature plateau of T_f (near 200 °C) is reached at t_f. The final stage (blue region) is reached as $\alpha \longrightarrow 1$, the optical absorption of the epoxy film saturates, the temperature stabilizes, and the epoxy is cured, at which point the laser illumination must be terminated to prevent charring.

Dependence on NP concentration, laser intensity

The model provides a useful qualitative comparison with experiments, allowing us to examine the effect of Au NP concentration (Fig. 3e, f), laser intensity (Fig. 3g, h), and other parameters (Appendix C) on photocuring dynamics. For increasing Au NP concentration (Fig. 3e, f), we predict an increase in T_p and a decrease in τ_p in a manner consistent with experimental observations. Interestingly, at the highest Au NP concentrations studied we observe a slight reduction in the rate of the final phase curing step and a small decrease in final temperature T_f. This seemingly paradoxical slowing is actually caused by the strong optical absorption produced by an excess of nanoparticles, which decreases laser transmission, slows the photocuring process, and suggests a slightly lower NP concentration of $\sim 2.2 \times 10^{10}$ cm^{-2} would be optimal. Since NP melting would abruptly quench a primary source of heating, the model shows that the smooth temporal evolution observed experimentally indicates the NPs remain intact throughout (see Appendix C for more).

When the NP concentration is kept constant, we observe an increase in T_p and a decrease in τ_p as laser intensity increases (Fig. 3g, h). The final phase curing rate increases consistently with increasing laser intensity, as does the final phase curing temperature T_f. This region of parameter space provides a clear path for reducing the time of the curing process; in this case, increasing the laser intensity from 5 W/cm^2 to 6.1 W/cm^2 reduces the total photocuring time by a factor of three.

While the theoretical model does not capture the experimental behavior with highly quantitative accuracy due to experimental variabilities such as non-uniform NP distribution, NP aggregation, and epoxy film aging (Appendix C), it is clearly highly capable of capturing qualitative trends that can provide paths to optimization for the photocuring process. We also investigated the influence of other relevant parameters like activation energies, effective aggregation coefficient, and air convection coefficient (Appendix C). Alternative, more cost effective

materials may be used instead of gold nanoparticles for larger scale processes. The case of aluminum nanoparticles is presented through theoretical calculations in Appendix D.

Bond strength measurements

An advantage of this technique is that by adding NPs to the epoxy film, heating is sufficiently concentrated in the epoxy to cure it with a laser power sufficiently reduced to prevent charring of the bonded composites. To investigate the structural qualities of the Au NP-activated photocured epoxy, we measured the strength of the bond formed by this process between two pieces of composite materials (Fig. 4). The epoxy film was placed between two composite "coupon" samples, and a laser welding of the lap joint was performed (see Appendix E for more details). For each sample, the joint was clamped at both ends prior to photocuring, and the temperature of the joint was controlled to follow a 30-minute ramp time to 177 °C (350 F), then held at this temperature for one hour. (Laser bonding and welding require continuous monitoring because these runaway processes can quickly damage the sample, so the laser power was manually decreased as the optical absorption of the epoxy layer increased.)

At laser powers sufficiently low to prevent charring (below 232 °C), the top composite sample absorbed approximately half the laser power at 532 nm, and approximately one third of the laser power reached the adhesive. Note that although the composite was sufficiently translucent for some laser illumination to reach the epoxy, the highly scattering composite was too opaque for the epoxy to be seen through the composite before or after the cure. Fig. 4b shows a thermal image of a coupon sample being bonded at an average temperature of 173 °C (343 F) with 10 W of 532-nm laser power whose unfocused ~1-mm diameter spot scanned in a 1″ × 1″ (2.5 cm × 2.5 cm) square pattern and produced an average illumination intensity of 1.55 W/cm^2. Outside the scanned regions, the temperature dropped rapidly to below 38 °C (100 F) only 1.6 cm away from the heated area. The composite temperature was linear with laser power with a slope of 16 °C/W for the range of laser power available.

After curing, the bonded samples were cooled and tested for bond strength by performing standard lap shear measurements (Instron 5569 universal test frame with 50 kN capacity, see Appendix E for more). For a bonding application, what matters most is the maximum load the junction can sustain, not the extension of the junction under a certain amount of load. The samples were pulled along the axis of the bond until the bond broke, indicated by the sudden decrease in load. FM 300 epoxy films with $\rho_{NP} = 0$, 5.5×10^9, 1.1×10^{10}, and 2.2×10^{10} NP/cm^2 were compared under identical conditions of sample clamping and illumination intensity ($I_L = 1.55$ W/cm^2), area (unfocused 10 W spot scanned over 1″ × 1″), and duration (30 min). In this comparative study, none of the bonds were completely photocured. The illumination was only 60% of the power needed to activate the FM 300 adhesive sandwiched between the coupon samples. In the lap shear strength data plotted in Fig. 4a, the three samples doped with NPs all show increased load strength over the undoped sample, and the NPs accelerated the cure rate so that the bond completed more of the annealing process within the 30 min of laser exposure. The most heavily doped sample ($\rho_{NP} = 2.2 \times 10^{10}$ NP/cm^2) failed at 1800 N (407 lbs), while the undoped sample failed at only 1300 N (286 lbs). (Additional information about bonding in the undoped case may be found in Appendix E.) For comparison, we performed the photocuring experiment on a sample with $\rho_{NP} = 2.2 \times 10^{10}$ NP/cm^2 Au NPs and allowed the photocuring process to complete. For the case of complete photocuring, a 4000 N (890 pound, ~2970 psi) load was supported before cleavage occurred. *This failure was caused not by a failure of the epoxy film but by a shearing failure of the composite sample itself.* Beyond this additional curing strength, a significant acceleration in curing rate

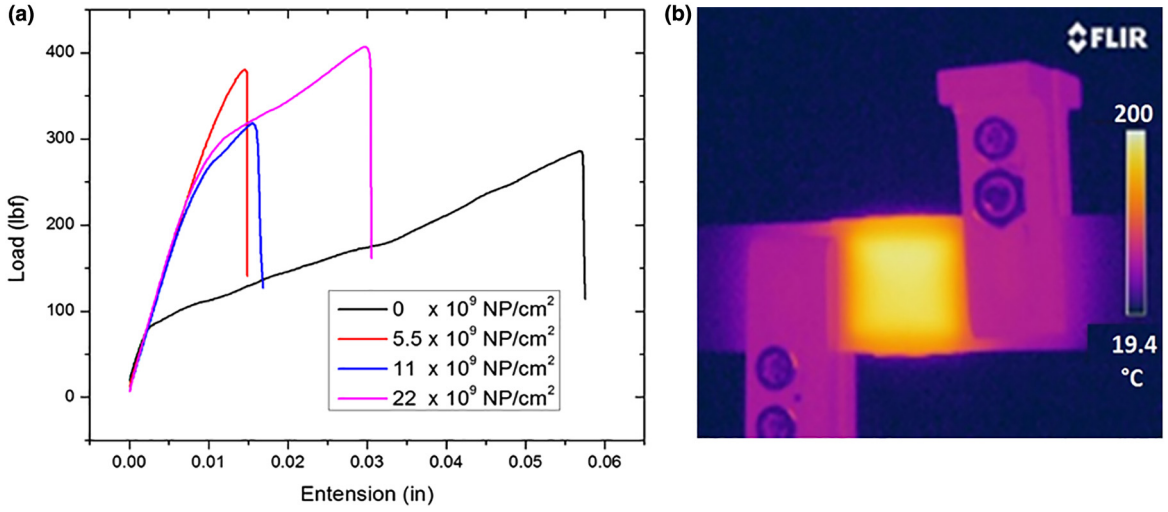

FIGURE 4

Lap shear measurements and photocured bond imaging. (a) Lap shear measurements for four samples of increasing nanoparticle concentration: 0, 5.5×10^9 NP/cm^2, 1.1×10^{10} NP/cm^2, and 2.2×10^{10} NP/cm^2, following identical photocuring conditions of laser intensity (1.55 W/cm^2), illumination area (1″ × 1″), and duration (30 min). (b) Infrared image of the photocuring bond formed between two pieces of composite material, showing mounting clamps to the left and right, during laser illumination.

is another substantial positive feature of the Au NP-based photocuring process. Comparing the curing rate of the best-case NP bond with the undoped case would suggest that the Au NPs enhance the curing rate of laser bonding by ~40%.

Conclusion

We have investigated how the laser bonding of composite materials using conventional heat-cured epoxy films can be enhanced by transforming conventional thermal curing into a plasmonic NP-based photocuring process. Au NPs, when incorporated into an epoxy film and illuminated at their plasmon resonance, substantially decrease the curing time relative to the conventional thermal curing process. Our studies focus on the important regime where plasmonic nanoparticle induced photothermal heating increases the optical absorption of the epoxy itself, so that both the nanoparticles and the photothermally modified epoxy drive the curing process. The kinetics of photocuring deviates quite dramatically from laser curing without nanoparticles and can be described by a four-stage process. A complex theoretical model was developed to understand this behavior, capturing the trends in photocuring kinetics observed for changes in NP concentration and laser intensity. This theoretical tool also helps ascertain possible optimization paths for this process, identifying regimes where the rate of photocuring can be significantly increased and producing a more efficient photocuring process. Bond strength measurements indicated that the nanoparticle-laden epoxies cured more quickly and strongly for a given illumination time and, when the photocuring process is complete, yield an epoxy bond even stronger than the composite material.

The analysis presented here clearly indicates that plasmonic nanoparticle-based photocuring is a highly attractive solution for the bonding of composite materials, providing several significant advantages to current oven-curing methods. This combination of faster curing rates, stronger bonds for composite material repair, and a localized, laser-based "spot welding" application, all point to this approach as a major improvement for the bonding or repair of composite materials. Further adaptation to other types of epoxies, and the possible use of earth abundant plasmonic nanoparticles, may facilitate the commercialization and widespread adoption of this process.

Acknowledgments

This work was partially supported by the Army's Aviation and Missile Research, Development, and Engineering Center. MER is supported through the Oak Ridge Institute for Science and Education. The authors thank Sean Thompson, David Busby, and Lance Hall for the lap shear measurements. PN and JY acknowledge support from the Robert A. Welch Foundation under Grant C-1222, and NJH acknowledges support from the Robert A. Welch Foundation under Grant C-1220. PN, NJH, and HOE all acknowledge the Air Force Office of Scientific Research Multidisciplinary Research Program of the University Research Initiative (MURI FA9550-15-1-0022).

Appendices A–E. Supplementary data

Supplementary data to this article can be found online at https://doi.org/10.1016/j.mattod.2018.09.005.

References

[1] K.K. Cha, Composite Materials: Science and Engineering, Springer Science & Business, Media, 2012.
[2] D. Gay, S.V. Hoa, Composite Materials: Design and Applications, second ed., CRC Press, 2007.
[3] E.J. Barbero, Introduction to Composite Materials Design, CRC Press, 2011.
[4] A. Chatterjee, J. Appl. Polym. Sci. 114 (2009) 1417–1425.
[5] D.H.-J.A. Lukaszewicz, C. Ward, K.D. Potter, Compos. Part B Eng. 43 (2012) 997–1009.
[6] H. Potente, O. Karger, G. Fiegler, Macromol. Mater. Eng. 287 (2002) 734–744.
[7] A.T. Roberts, H.O. Everitt, Nanoparticle Assisted Laser Bonding in Composites. U.S. Army AMRDEC Tech. Reports RDMR-WD-15-17 2015, 1–30.
[8] J. Dong et al., Nanotechnology 28 (2017) 0065601.
[9] C.I. Evans et al., Nano Lett. 17 (2017) 5646–5652.
[10] A. Alabastri et al., Nano Lett. 17 (2017) 5472–5480.
[11] P. Zolotavin et al., ACS Nano 10 (2016) 6972–6979.
[12] A. Alabastri et al., Materials 6 (2013) 4879–4910.
[13] A. Alabastri et al., ACS Photonics 2 (2015) 115–120.
[14] A.B. Taylor, A.M. Siddiquee, J.W.M. Chon, ACS Nano 8 (2014) 12071–12079.
[15] L. Jonušauskas et al., Nanotechnology 27 (2016) 154001.
[16] FM 300 Epoxy Film Adhesive data sheet https://www.cytec.com/sites/default/files/datasheets/FM_300_081211-08a.pdf.
[17] J. Zhang, Y. Xu, P. Huang, e-Polymers 10 (2010) 2197–4586.
[18] L. Sun, Thermal Rheological Analysis of Cure Process of Epoxy Prepreg, Doctoral Thesis, Louisiana State University, 2002.
[19] G.L. Hagnauer, B.R. LaLiberte, D.A. Dunn, in: Epoxy Resin Chemistry II; ACS Symposium Series, American Chemical Society, 1983, pp. 12–229.
[20] K. Horie et al., J. Polym. Sci. Part A-1 Polym. Chem. 8 (1970) 1357–1372.
[21] M.A. Acitelli, R.B. Prime, E. Sacher, Polymer (Guildf). 12 (1971) 335–343.
[22] R.B. Prime, E. Sacher, Polymer (Guildf) 13 (1972) 455–458.